

The Novel Silatecan 7-*tert*-Butyldimethylsilyl-10-hydroxycamptothecin Displays High Lipophilicity, Improved Human Blood Stability, and Potent Anticancer Activity

David Bom,[†] Dennis P. Curran,[†] Stefan Kruszewski,[‡] Stephen G. Zimmer,^{§,||} J. Thompson Strode,[‡] Glenda Kohlhaugen,[⊥] Wu Du,[†] Ashok J. Chavan,[#] Kimberly A. Fraley,[‡] Alex L. Bingcang,[‡] Lori J. Latus,[#] Yves Pommier,[⊥] and Thomas G. Burke^{*,‡,||,‡}

Department of Chemistry, University of Pittsburgh, Pittsburgh, Pennsylvania 15260; Division of Pharmaceutics Sciences, College of Pharmacy, Department of Microbiology and Immunology, College of Medicine, and Experimental Therapeutics Program, Markey Cancer Center, University of Kentucky, Lexington, Kentucky 40506; Molecular Pharmacology Program, National Cancer Institute, Bethesda, Maryland 20892; and Tigen Pharmaceuticals, Inc., Lexington, Kentucky 40506

Received March 28, 2000

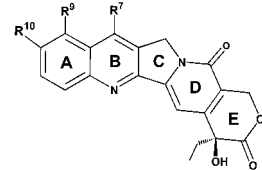
We describe the rational design and synthesis of B- and A,B-ring-modified camptothecins. The key α -hydroxy- δ -lactone pharmacophore in 7-*tert*-butyldimethylsilyl-10-hydroxycamptothecin (DB-67, **14**) displays superior stability in human blood when compared with clinically relevant camptothecin analogues. In human blood **14** displayed a $t_{1/2}$ of 130 min and a percent lactone at equilibrium value of 30%. The *tert*-butyldimethylsilyl group renders the new agent 25-times more lipophilic than camptothecin, and **14** is readily incorporated, as its active lactone form, into cellular and liposomal bilayers. In addition, the dual 7-alkylsilyl and 10-hydroxy substitution in **14** enhances drug stability in the presence of human serum albumin. Thus, the net lipophilicity and the altered human serum albumin interactions together function to promote the enhanced blood stability. In vitro cytotoxicity assays using multiple different cell lines derived from eight distinct tumor types indicate that **14** is of comparable potency to camptothecin and 10-hydroxycamptothecin, as well as the FDA-approved camptothecin analogues topotecan and CPT-11. In addition, cell-free cleavage assays reveal that **14** is highly active and forms more stable top1 cleavage complexes than camptothecin or SN-38. The impressive blood stability and cytotoxicity profiles for **14** strongly suggest that it is an excellent candidate for additional in vivo pharmacological and efficacy studies.

Introduction

Camptosar (CPT-11) and Hycamtin (topotecan, TPT) (Table 1) are the first two drugs in the camptothecin family to gain FDA approval, and they are now being used in the clinic to treat certain types of solid tumors. Like all camptothecins, these drugs function by inhibiting DNA topoisomerase I (top1).^{1–4} Because the camptothecins are S-phase-specific drugs,^{5–8} optimal top1 inhibitory activity is only obtained when the tumors of a patient are exposed to the drugs for continuous periods of time.⁹ In addition, structure–activity studies (SAR) show that successful inhibition of top1 by camptothecins requires an intact lactone ring (ring E) functionality.^{10–13}

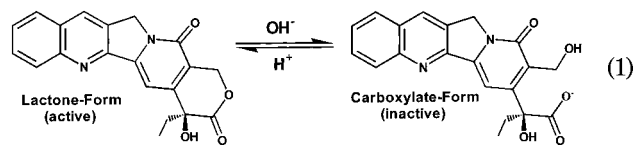
The pharmaceutical development and clinical utility of the camptothecins are limited by the distinctive dynamics of these agents in the bloodstream. All of the camptothecins now in clinical development contain an α -hydroxy- δ -lactone, and they exist in two distinct forms at physiological pH of 7.0 and above. As shown in eq 1, the biologically active “lactone-closed” form reacts with

Table 1. Structure of Camptothecin and Its Analogues



compd	R ⁷	R ⁹	R ¹⁰
camptothecin	H	H	H
SN-38	C ₂ H ₅	H	H
topotecan	H	CH ₂ N(CH ₃) ₂	OH
15	Si(CH ₃) ₂ (CH ₂) ₄ Cl	H	H
17	Si(CH ₃) ₂ (CH ₂) ₄ Cl	H	OH
12	Si(CH ₃) ₂ C(CH ₃) ₃	H	H
14	Si(CH ₃) ₂ C(CH ₃) ₃	H	OH

water to form a biologically inactive^{10,13,14} “lactone-opened” (carboxylate) form:



This simple chemical hydrolysis dynamically inactivates the parent drug.¹⁵ The hydrolysis problem with camptothecin and many analogues is exacerbated in human blood because the predominant blood serum protein,

* Correspondence to: Thomas G. Burke, Ph.D., The University of Kentucky, AStCC Building, Lexington, KY 40506. Phone: (606) 257-2300, ext. 255. Fax: (606) 257-2489. E-mail: tgburke@pop.uky.edu.

[†] University of Pittsburgh.

[‡] Division of Pharmaceutics Sciences, University of Kentucky.

[§] Department of Microbiology and Immunology, University of Kentucky.

^{||} Experimental Therapeutics Program, University of Kentucky.

[⊥] National Cancer Institute.

[#] Tigen Pharmaceuticals, Inc.

albumin, preferentially binds to the carboxylate form. This shifts the lactone/carboxylate equilibrium toward the inactive carboxylate.^{16–18} Accordingly, establishing conditions where a therapeutically relevant concentration of the lactone-closed form of a camptothecin is present over a suitable period of time for tumor cells to cycle through the S-phase is a major challenge.

The hydrolysis reaction and the ability of human serum albumin (HSA) to strongly bind the carboxylate form of drugs such as camptothecin and 9-aminocamptothecin (9-AC) are transitionally relevant. For example, 9-AC administered intravenously is useful in treating brain cancer in murine animal models. However, the pharmacokinetic behavior of these agents in mice is markedly different from that in humans.^{17,18} We have shown that camptothecin lactone levels are about 100-fold greater in mouse blood than in human blood due to reduced binding of the carboxylate form to mouse albumin. It follows that the amount of free lactone form of the drug available to cross membrane systems, such as the blood–brain barrier, is probably about 100-fold lower in humans. Of 99 brain cancer patients, treated with 9-AC administered intravenously,¹⁹ only 1 showed a partial response. Our physical data suggest an explanation for this disappointing ineffectiveness: promptly after administration, more than 99.5% of the active drug is converted to the inactive carboxylate form, which is in turn bound to HSA. Most of the intravenously administered 9-AC is protein-bound and unavailable to cross the blood–brain barrier or reach the primary tumor lesion by other means.

In 1996, our research groups initiated a collaboration with the goal of discovering camptothecins that display improved human blood stability. We hypothesized that stabilizing the lactone-closed form was the key to realizing this goal. We sought to stabilize the lactone by introducing substituents that would promote partitioning into the lipid bilayer (hence protecting the drug from hydrolysis)^{17,20} or that would interfere with the binding of the derived camptothecin carboxylate to HSA (hence preventing the shift in equilibrium toward the inactive form). DNA interactions (both single- and double-stranded) in the absence of DNA top1 have been shown to stabilize the lactone form of camptothecins.²¹ Our current work represents a rational design approach to optimizing circulating lactone levels by enhancing lipophilicity and reducing the high-affinity binding of camptothecin carboxylate for human albumin. For the time being we have omitted, for the sake of simplicity, structural design considerations aimed at optimizing the interactions of the lactone forms of camptothecins with DNA.

Data from several labs encourage the development of lipophilic camptothecin analogues. Yves Pommier and colleagues at the National Cancer Institute have shown that intrinsic potencies against the top1 target are markedly higher for lipophilic camptothecins when compared to the water-soluble, FDA-approved agents.²² Similarly, Dr. Beppino Giovanella of the Stehlin Foundation has observed improved activities of lipophilic camptothecin analogues, such as 9-nitrocampthothecin, over water-soluble analogues in murine models *in vivo*.⁸

We have also shown that camptothecin and 9-AC exhibit poor stabilities in human blood due to the high-

affinity, noncovalent binding interaction of their carboxylate forms with HSA.¹⁶ Frequency-domain lifetime fluorometry measurements reveal that HSA preferentially binds camptothecin carboxylate with over a 100-fold higher affinity than camptothecin lactone.¹⁷ The selective binding of carboxylate over lactone shifts the hydrolysis equilibrium to favor the inactive carboxylate. In solutions containing HSA as well as and in human plasma, camptothecin and 9-AC open rapidly and only negligible amounts of lactone (~0.2%) remain at equilibrium. However, not all camptothecin congeners are negatively affected by preferential carboxylate binding to HSA. For example, the carboxylate form of topotecan (a 9,10-disubstituted camptothecin) does not bind with high affinity to HSA.^{23,24} Our structure/function data reveal that dual substitution at the 7,10-positions effectively ablates high-affinity binding of the carboxylate form to HSA.²³ An example of a drug that exhibits this ablation is SN-38 (the active component of irinotecan or Camptosar), which is 7-ethyl-10-hydroxycamptothecin. This emerging understanding of the molecular basis for lactone ring stability in the presence of HSA plays a central role in discovering new analogues that exhibit improved lactone ring stability in human blood.

In 1997, we reported the radical-mediated preparation of about two dozen 7-silylcampthothecins (silatecans). Many of these silatecans displayed good *in vitro* activity against the HL-60, 833K, and DC-3F cell lines.²⁵ The flexibility and generality of the cascade radical annulation approach have enabled us to prepare several hundred new silatecan and homosilatecans for biological evaluation.^{26,27} Among the silatecan series, DB-67 (7-*tert*-butyldimethylsilyl-10-hydroxycamptothecin, **14**) is emerging as a serious candidate for cancer chemotherapy. The studies reported herein show that **14** is significantly more blood-stable than clinically relevant existing camptothecin analogues and that it possesses high intrinsic potency against top1 and impressive anticancer activity both *in vitro* and *in vivo*.²⁸

Results and Discussion

The synthetic approach to **12**, **14**, **15**, and **17** is elaborated in Scheme 1. The anion of tetrahydropyranyl ether **1** was silylated with the appropriate chlorosilane to give silyltetrahydropyranyl ethers **2** and **3** (not shown) in 92% and 89% yields. Subsequent bromination with PPh₃/Br₂ gave propargyl bromides **4** and **5** in 91% and 72% yields. Iodopyridone **6** was *N*-alkylated with propargyl bromide **4** under the standard conditions²⁹ to give **7** in 77% yield. Applying the same *N*-alkylation conditions to **5** resulted in a 54% yield of a 1.6:1 ratio of an undesired bromopropyl byproduct **9** and the desired chloropropyl pyridone **8**, as determined from the ¹H NMR spectrum. Substitution of LiBr with LiCl in the *N*-alkylation of **5** resulted in a 50% yield of **8** containing only 7% contamination by **9**. Cascade cyclization^{26,27} of **7** and **8** with isonitriles **10** and **11** gave the four camptothecin analogues **12**, **13**, **15**, and **16** in 54%, 41%, 53%, and 45% yields. Deprotection of **13** and **16** using K₂CO₃ gave the free phenols **14** and **17** in 85% and 44% yields.

Several analytical and biophysical methods were employed to compare the blood component interactions and blood stabilities of the new silatecans with those of

DMPC and DMPG bilayers.²⁰ The association constants for water-soluble topotecan ($K_{\text{DMPC}} = 10 \text{ M}^{-1}$ and $K_{\text{DMPG}} = 50 \text{ M}^{-1}$) are less than the values noted for camptothecin.²⁰ The data contained in Figure 1 and summarized in Table 2 indicate that a marked enhancement of the membrane partition coefficient can be achieved through 7-silylalkyl or dual 7-silylalkyl-10-hydroxy substitution.

Silatecan **12**, which contains a 7-*tert*-butyldimethylsilyl functionality, displays the highest lipophilicity of any of the silatecans studied ($K_{\text{DMPC}} = 15\,500 \text{ M}^{-1}$ and $K_{\text{DMPG}} = 16\,000 \text{ M}^{-1}$). Comparison of the association constants for **12** and **14** and **15** and **17** reveals that insertion of a 10-hydroxy functionality significantly reduces membrane binding. In the case of **12**, addition of a 10-hydroxy functionality, to form **14**, resulted in an approximate 6-fold change; while in the case of **15**, 10-hydroxy addition (i.e. **17**) produced only a 2-fold change. Nonetheless, **14** is a highly lipophilic agent compared to clinically relevant camptothecins. Analogue **14** is 25-times more lipophilic than camptothecin, 10-times more lipophilic than SN-38, and 250-times more lipophilic than topotecan in suspensions composed of DMPC. Overall, our data indicate that addition of silylalkyl functionalities at the 7-position provides a convenient and effective means of varying the lipophilicity of the silatecans over a wide range.

Direct evidence of extensive partitioning of **14** into red blood cells is depicted in Figure 1 of Supporting Information. Silatecan **14** as well as SN-38 exhibit marked spectral shifts in their emission spectra when they partition from water to a nonaqueous environment such as an organic solvent or lipid bilayer. Panels a and d of the Supporting Information figure show the spectral shifting for **14** and SN-38, respectively. In panels b and e, the recorded emission spectra of **14** and SN-38 at drug concentrations of 10 and 50 μM in a suspension of red blood cells are shown. Panels c (**14**) and f (SN-38) compare spectra (maxima of each normalized to unity) of 10 μM drug in PBS solution versus drug in suspensions of red cells. The spectral shifting for **14** in the presence of RBCs (panel c) is more prominent than for SN-38 (panel f). Thus, the red cell partitioning of **14** (panel c) is much more extensive than observed for SN-38 (panel f), a finding which is consistent with our model membrane binding data summarized in the Supporting Information which shows that SN-38 is 10-times less lipophilic than **14**.

In addition to displaying markedly higher lipophilicities relative to the conventional camptothecins (i.e. camptothecin, topotecan), **14** exhibited superior human blood stability. Figure 2 depicts the stabilities of the four novel silatecans in solutions of phosphate-buffered saline (PBS) at a pH value of 7.4 (left panel) and in human blood (right panel). In PBS, the silatecans as well as clinically relevant camptothecins show approximately 10–15% lactone remaining at equilibrium. Drug stability in human blood is of the most significance, and **14** displays by far the best stability in this matrix. Figure 2, right panel, depicts the human blood stabilities of the four novel silatecans and the pronounced effect which dual 7-silylalkyl-10-hydroxy substitution has on promoting high lactone levels. Human blood stability parameters for the new silatecans are summarized in Table 3. The greater than 30% lactone

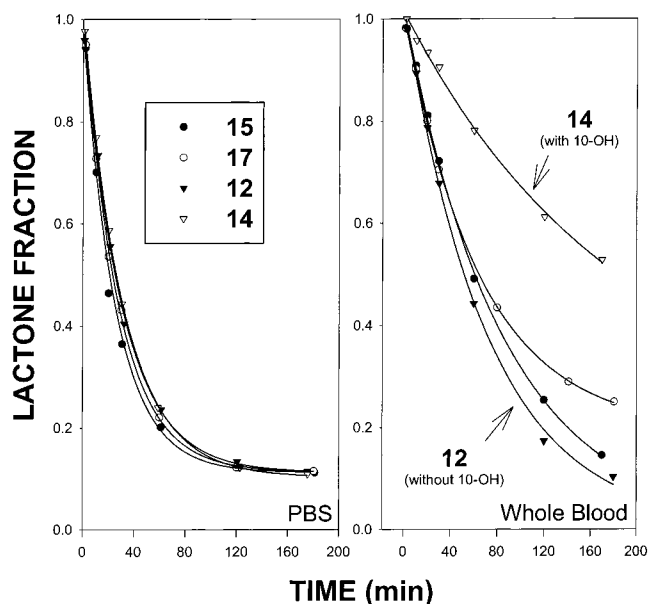


Figure 2. Depiction of the improved human blood stability of **14** in PBS (left panel, 1 μM drug concentration) and in human blood (right panel, 1 μM drug concentration) relative to a series of other silatecans that include **15**, **17**, and **12**. While each of the silatecans exhibited similar hydrolysis profiles in PBS solution, large differences in stability were observed in human blood with **14** being the most blood-stable silatecan of the group. Stability profiles were determined using HPLC methods. All experiments were conducted at pH 7.4 and 37 °C. Each data point represents the average of three or more determinations with uncertainty of 10% or less. Stability parameters are summarized in Table 3.

Table 3. Summary of Kinetic and Equilibrium Parameters for the Hydrolysis of Camptothecin Drugs in Human Blood, PBS, PBS with HSA, and PBS with RBC^a

compd	solution or suspension	$t_{1/2}$ (min)	% lactone at
12	whole blood	71.0 ± 4.2	1.0 ± 0.1
	PBS with HSA	46.3 ± 1.0	0.1 ± 0.2
	PBS only	27.9 ± 1.9	12.2 ± 0.4
	PBS with RBC	79.4 ± 3.3	59.4 ± 0.0
14	whole blood	133.0 ± 15.9	30.5 ± 1.9
	PBS with HSA	119.0 ± 5.3	10.5 ± 2.0
	PBS only	31.8 ± 0.4	10.2 ± 0.3
	PBS with RBC	51.4 ± 0.5	41.4 ± 0.7
15	whole blood	85.6 ± 9.2	2.2 ± 3.6
	PBS with HSA	16.0 ± 0.2	2.7 ± 0.5
	PBS only	23.3 ± 2.4	12.0 ± 0.5
	PBS with RBC	59.7 ± 2.0	43.4 ± 0.8
17	whole blood	65.3 ± 9.0	17.8 ± 2.0
	PBS with HSA	48.0 ± 0.9	17.2 ± 0.7
	PBS only	29.5 ± 1.7	11.3 ± 1.8
	PBS with RBC	67.7 ± 8.5	50.2 ± 1.7
SN-38	whole blood	32.0 ± 2.3	19.5 ± 1.8
	PBS with HSA	36.1 ± 1.5	36.0 ± 0.0
	PBS only	20.9 ± 2.5	15.3 ± 1.7
	PBS with RBC	24.4 ± 2.6	37.5 ± 2.0
camptothecin	whole blood	21.6 ± 2.6	5.3 ± 0.6
	PBS with HSA	11.9 ± 0.3	<0.5
	PBS only	23.8 ± 1.3	17.0 ± 2.0
	PBS with RBC	30.8 ± 2.8	34.6 ± 1.0

^a Hydrolysis parameters were determined using HPLC assays. Drug concentrations of 1 μM were employed. Drug samples were incubated in blood or PBS (pH 7.4) either with or without physiologically relevant concentrations of HSA or RBC. All experiments were conducted at 37 °C.

at equilibrium value for **14** compares very favorably to the corresponding percent lactone levels in whole human blood for 9-AC (~1%), camptothecin (~5%), topo-

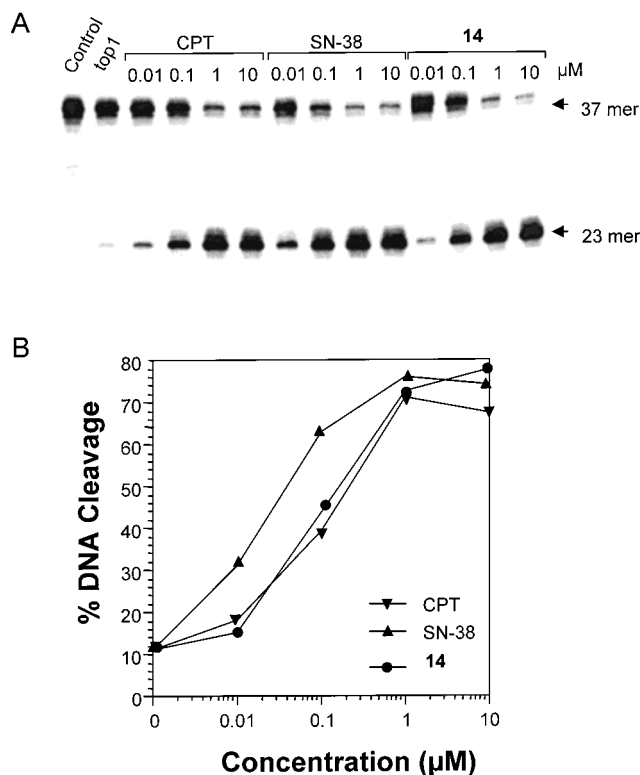


Figure 3. Top1-induced DNA cleavage caused by **14** in the top1 oligonucleotide. Reactions were for 30 min at room temperature and were stopped by adding 0.5% SDS: (A) phosphorimager picture of the gel (drug concentrations are indicated above lanes); (B) quantitation of the results shown in panel A.

tecans (~12%), CPT-11 (~21.0%), and SN-38 (~20%). Within the silatecan family of agents, the percent lactone at equilibrium value for **14** is 30.5% in comparison to 2.2% (**15**), 17.8% (**17**), and 1.0% (**12**) for the other silatecans. As analogue **12** is identical to **14** with the exception that it is unsubstituted at the 10-position; the 10-hydroxy substitution thus appears to be a key factor in elevating active lactone levels. Likewise, **17** also exhibits improved stability in whole blood relative to its unsubstituted counterpart, **15**. The dual 7-silylalkyl-10-hydroxy-substituted agents, **14** and **17**, display good stability both in the presence of physiologically relevant concentrations of HSA as well as in the suspensions containing physiologically relevant concentrations [$(5 \pm 1) \times 10^6$ cell/ μ L] of albumin-free red blood cells. Drug stability in red cell suspensions is consistent with the notion that the lactone form of these agents readily partitions into erythrocyte membranes and is thereby protected from hydrolysis. Thus, the 10-hydroxy group and the drug lipophilicity together enhance the stability of **14**.

On the basis of its superior human blood stability, **14** was selected for extensive pharmacological testing. Figures 3–5 illustrate the high intrinsic top1 inhibitory activity of **14** in cell-free assays. Top1-induced DNA cleavage caused by **14** in the top1 oligonucleotide is presented in Figure 3. The percent DNA cleavage for **14** exceeded the value for camptothecin and was less than that observed for SN-38. Figure 4 is a comparison of top1-induced DNA cleavage caused by the novel silatecans, SN-38 and camptothecin (CPT). The silatecans were found to be highly active and of comparable

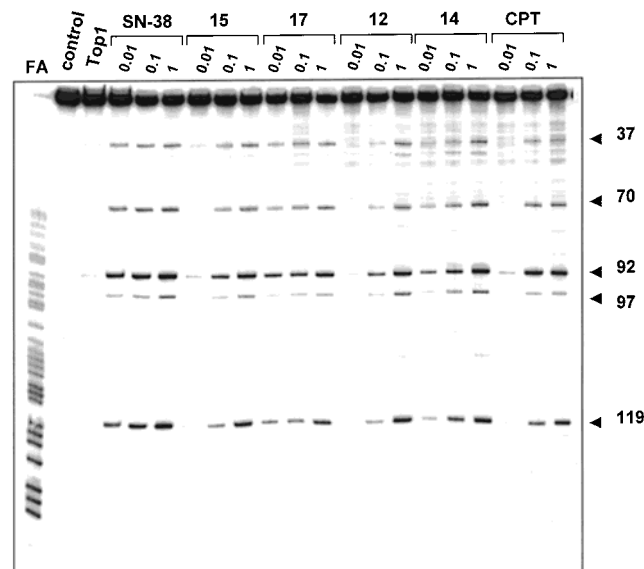


Figure 4. Comparison of top1-induced DNA cleavage induced by the novel camptothecin derivatives, SN-38, and camptothecin (CPT). The DNA fragment used corresponds to the 3'-end-labeled *PvuII/HindIII* fragment of pBluescript SK(-) phagemid DNA. Reactions were for 30 min at room temperature and were stopped by adding 0.5% SDS. Drug concentrations are indicated above lanes. DNA fragments were separated on 16% polyacrylamide gels FA: purine ladder. The numbers to the right correspond to the top1-mediated DNA cleavage sites induced by the drugs.

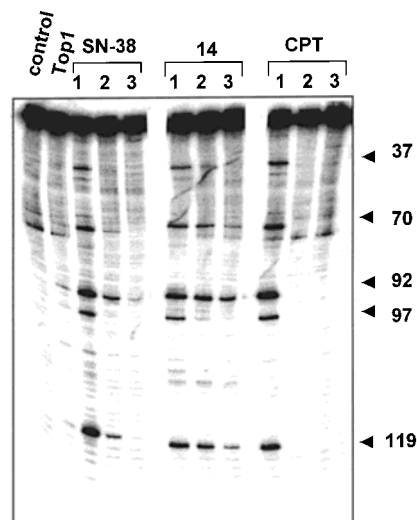


Figure 5. Stability of the top1 cleavage complexes induced by **14**. The DNA fragment is the same as in Figure 5. After a 30-min reaction with top1, a reaction aliquot was stopped with 0.5% SDS (lanes 1) and NaCl was added to the rest of the reactions to a final concentration of 0.35 M. Aliquots were then taken after an additional 15 min (lanes 2) and 30 min (lanes 3).

potency relative to camptothecin and SN-38. Figure 5 illustrates the stability of the top1 cleavage complexes induced by **14** relative to the other agents of interest. The results indicate that in the presence of **14** very stable top1 cleavage complexes are formed. The top1 cleavage complexes trapped by **14** are more stable than those trapped by camptothecin or even SN-38, which we previously reported to induce more stable cleavage complexes than camptothecin.^{30,31} Overall, the cell-free cleavage assays reveal that **14** is highly active, forming very stable top1 cleavable complexes.

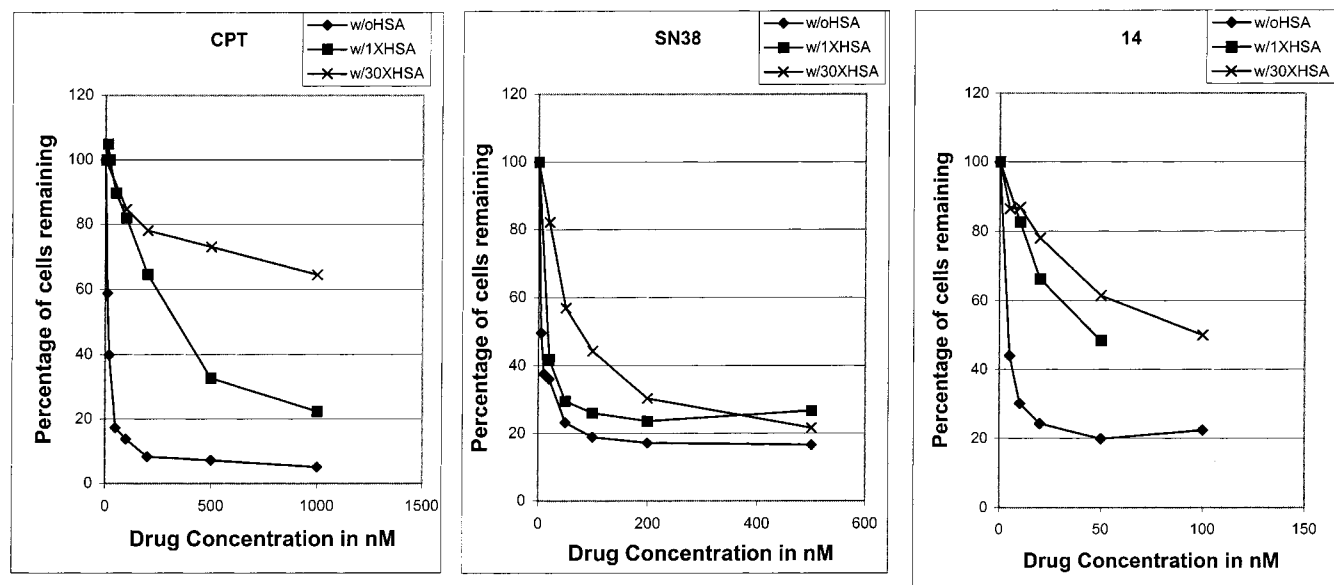


Figure 6. Impact of HSA on the anticancer activities of camptothecin, SN-38, and **14**. The studies were conducted with MDA-MB-435 human breast cancer cells. The HSA concentrations were 1 and 30 mg/mL. Normal HSA levels in the human range from 30 to 50 mg/mL. Thus, physiologically relevant levels of human albumin markedly ablate the anticancer activities of the parent agent as well as several other camptothecin analogues (data not shown). These effects are not nearly as strong for 7,10-substituted agents such as SN-38 or **14**.

The cytotoxic potency of **14** was tested against a variety of human tumor cell lines derived from several different tumor types (non-small-cell lung cancer, ovarian cancer, breast cancer, melanoma, etc.) in the NCI cytotoxicity screen. For comparative purposes, we evaluated the cytotoxic activities of **14** relative to camptothecin, 10-hydroxycamptothecin, SN-38, and topotecan. Topotecan has been FDA-approved as a second-line treatment for ovarian and lung cancer, while SN-38, the active agent of the FDA-approved prodrug CPT-11, is used as a first-line therapy for the treatment of colon cancer. The *in vitro* cytotoxic potency of **14** is comparable or slightly enhanced relative to camptothecin and 10-hydroxycamptothecin. The mean GI_{50} value of **14** is in the 21 nM range as compared to 44 and 36 nM values for camptothecin and 10-hydroxycamptothecin, respectively. Compared with topotecan, **14** displays similar cytotoxic potency values for ovarian, colon, prostate, and breast cancers. However, as the GI_{50} value was never realized against several of the cell lines, in particular non-small-cell lung cancer, CNS cancer, renal cancer, leukemia, and melanoma lines, the data suggest that for several tumor types **14** may possess equivalent or superior potency relative to topotecan. Although the mean GI_{50} value for **14** indicates a negligible reduction in potency in comparison to topotecan (21 nM vs 11 nM, respectively), it is important to note that over half of the GI_{50} values for **14** registered less than the 10 nM range and, accordingly, could not be factored into the mean GI_{50} value. With respect to SN-38, the general trend among the different cell lines suggests that **14** has a cytotoxic potency that is approximately 1 order of magnitude less than that of SN-38; indeed, the mean GI_{50} values for **14** and SN-38, 21 nM vs 2 nM, respectively, reflect this trend.

Previous literature results have indicated that HSA is capable of strongly modulating the anticancer activities of camptothecin.²⁴ Consequently, we conducted cytotoxicity measurements in the absence and presence of

HSA. Figure 6 indicates that the activity of camptothecin against MDA-MB-435 S human breast cancer cells is markedly decreased by the presence of HSA. In the absence of HSA, camptothecin exhibited an IC_{50} value of 15 nM, which increased markedly to 375 nM with the addition of a very dilute concentration of 1 mg/mL HSA. At a more physiologically relevant concentration of 30 mg/mL, essentially only very low levels of activity were observed even at drug concentrations as large as 1 μ M (Figure 6). Interestingly, the impact of HSA on anticancer activities of 7,10-substituted agents (i.e. SN-38 or **14**) was not nearly as strong. In the absence of albumin, the IC_{50} values for **14** and SN-38 were 14 and 5 nM, respectively. At an HSA concentration of 30 mg/mL, SN-38 exhibited an IC_{50} value of 50 nM, while the IC_{50} value for **14** was increased to 90 nM. This relatively modest drop in IC_{50} value to 90 nM for **14** is likely due to nonspecific binding of drug by albumin. However, the effect of HSA on the activity of **14** is not nearly as strong as the effect of the protein on the activities of camptothecin and other analogues such as 9-AC.

Overall, the above data indicate that the cytotoxicity of **14** resides within a similar range as the two FDA-approved analogues, SN-38 and topotecan. Conclusions drawn from these *in vitro* assays do not take into account the complexities of camptothecin analogue dynamics *in vivo*. The data indicate that **14** displays enhanced stability in whole blood relative to SN-38 and topotecan. This significant increase in stability is in large part due to the net lipophilicity of analogue **14**; the lactone form can partition into biological membranes and thereby be protected from hydrolysis in the surrounding aqueous milieu. Although this lipophilicity factor cannot be addressed in our *in vitro* assays, it is reasonable to postulate that the lipophilicity of **14** *in vivo* may function to augment its cytotoxic potency.

In support of this postulated enhanced *in vivo* potency are data showing that **14** is efficacious in treating

murine xenograft models.²⁸ A dose-escalation study of this agent in a nude mouse U87 glioma subcutaneous model system demonstrated a concentration-dependent effect, with tumor growth inhibition at day 28 postimplantation (the day control animals began to require sacrifice due to large tumor size) of 61% and 73% after administration of **14** at doses of 3 and 10 mg/kg/day, respectively, for 5 days beginning on postimplantation day 7. Animals that continued treatment with 10 mg/kg/day in three additional 21-day cycles all remained progression free after >90 days of followup (but later developed enlarging tumors after treatment was stopped). Interestingly, a slightly higher dose (30 mg/kg/day) induced complete tumor regression after only two cycles in all study animals and was effective even if treatment was delayed until large, bulky tumors had developed. Application of the 30 mg/kg/day dose to treat established intracranial glioma xenografts led to long-term (>120-day) survival in six of six animals, whereas all controls died of progressive disease. No apparent toxicity was encountered in any of the animals treated with **14**.

In summary, **14** is an excellent candidate for preclinical development. Silatecan (**14**) displays superior human blood stability relative to FDA-approved camptothecin agents, which is likely due to its high lipophilicity and reduced interactions with the high-affinity carboxylate binding site on HSA. Analogue **14** also possesses a very high intrinsic potency against the top1 target enzyme with a unique DNA cleavage profile. Thus, the combination of its potency and stability profiles suggests that it may be more efficacious than the currently used camptothecin-based therapies. In support of this we have presented in vivo murine data elsewhere²⁸ that reveal **14** can effectively cure mice of intracranially implanted human gliomas. Due to its outstanding activity in combination with its high human blood stability, **14** is a promising experimental agent for the treatment of human cancer.

Experimental Section

Caution. Camptothecin and related analogues are known to exhibit a variety of pharmacological properties; these materials should be labeled, handled, and disposed of properly.

Materials. IR spectra were recorded on an ATI Mattson Genesis Series FTIR. ¹H and ¹³C NMR data were collected on a Bruker AF-300 at 300/75 MHz or a DRX500 at 500/125 MHz. Low- and high-resolution mass spectra were obtained on a Fisons VG 7070 E or a Fisons VG Autospec, respectively. Flash chromatography was done on 60 Å silica gel (ICN Biomedicals). THF was obtained dry by distillation from Na/benzophenone. Dichloromethane and dimethoxyethane were distilled from NaH. All other reagents were used as received.

tert-Butyldimethyl(tetrahydropyran-2-yloxy)prop-1-ynylsilane (2). Tetrahydro-2-(2-propynyloxy)-2H-pyran (**1**) (15 g, 107 mmol) and THF (300 mL) were added to a flame-dried flask. The mixture was cooled to -78 °C and BuLi (70.2 mL, 112.3 mmol) was added. After 1 h, the mixture was quenched with *tert*-butyldimethylchlorosilane (17.8 g, 117.9 mmol) and warmed to room temperature. After 4 h at 22 °C, saturated NH₄Cl (150 mL) was added and the mixture was extracted with ether (2 × 300 mL). The organic layers were combined and dried (MgSO₄). After concentration, the crude oil was purified by filtration through a pad of silica gel (95:5 hex/EtOAc). Evaporation of the solvent gave the silyl ether **2** (25 g, 92%) as a clear oil: IR (CHCl₃, cm⁻¹) 683, 776, 826, 1030, 1122, 1251, 1389, 1470, 2175, 2856, 2947; ¹H NMR (300 MHz, CDCl₃) δ 0.09 (s, 6 H), 0.91 (s, 9 H), 1.42–1.90 (m, 6 H), 3.42–3.56 (m, 1 H), 3.77–3.89 (m, 1 H), 4.25 (s, 2 H), 4.80–4.88 (br

s, 1 H); ¹³C NMR (75 MHz, CDCl₃) δ -4.7, 16.4, 19.0, 25.3, 26.0, 30.2, 54.6, 61.9, 89.0, 96.4, 102.1; HRMS (EI) *m/z* calcd for (M - C₄H₉) C₁₀H₁₇O₂Si (M⁺) 197.0998, found 197.0992; LRMS (EI) *m/z* 197 (M - C₄H₉), 179, 159, 153, 139, 131, 125, 113, 103, 97, 85, 75, 57.

3-Chloropropyltrimethyl(tetrahydropyran-2-yloxy)prop-1-ynylsilane (3). Following the procedure outlined above, tetrahydro-2-(2-propynyloxy)-2H-pyran (**1**) (2.0 g, 14.3 mmol), THF (100 mL), *n*-BuLi (9 mL, 14.4 mmol) and chloropropyltrimethylchlorosilane (2.5 g, 14.4 mmol) were combined to give the desired silyl ether **3** (3.5 g, 89%) as a clear oil: IR (CHCl₃, cm⁻¹) 784, 817, 834, 868, 902, 993, 1033, 1060, 1078, 1121, 1201, 1253, 1343, 1441, 2175, 2853, 2871, 2901, 2956; ¹H NMR (300 MHz, CDCl₃) δ 0.18 (s, 6 H), 0.65–0.78 (m, 2 H), 1.45–1.92 (m, 8 H), 3.45–3.62 (m, 3 H), 3.78–3.90 (m, 1 H), 4.23 (d, *J* = 16 Hz, 1 H), 4.30 (d, *J* = 16 Hz, 1 H), 4.81 (t, *J* = 3 Hz, 1 H); ¹³C NMR (75 MHz, CDCl₃) δ -1.9, 13.6, 18.9, 25.3, 27.4, 30.2, 47.6, 54.6, 61.9, 89.2, 96.7, 102.6; LRMS (isobutane CI) *m/z* 275 (M⁺), 197, 159, 135, 93, 85.

3-tert-Butyldimethylsilyl-2-propynyl Bromide (4). Triphenylphosphine (16.2 g, 61.9 mmol) and dry CH₂Cl₂ (250 mL) were added to a flame-dried flask and the mixture was cooled to 0 °C. Next, Br₂ (9.4 g, 59 mmol) was added dropwise followed by a small amount of Ph₃P to be certain that no unreacted Br₂ remained. After 30 min, the silyl ether **2** (15 g, 59 mmol) was added. After 5 h at 0 °C, the mixture was diluted with H₂O and extracted with pentane (2 × 300 mL). The organic layer was washed with saturated NaHCO₃ (200 mL), dried (MgSO₄) and concentrated to 150 mL. This mixture was passed through a pad of silica gel using pentane (2 × 200 mL). Careful evaporation of the pentane gave the desired propargyl bromide **4** (12.6 g, 91%) as a clear oil: IR (CHCl₃, cm⁻¹) 682, 940, 1038, 1204, 1252, 1362, 1470, 2178, 2858, 2895, 2932, 2953; ¹H NMR (300 MHz, CDCl₃) δ 0.12 (s, 6 H), 0.95 (s, 9 H), 3.93 (s, 2 H); ¹³C NMR (75 MHz, CDCl₃) δ -4.9, 14.8, 16.6, 26.0, 90.8, 100.5; HRMS (EI) *m/z* calcd for C₉H₁₇BrSi (M⁺) 232.0283, found 232.0278; LRMS (EI) *m/z* 232 (M⁺), 177, 175, 149, 147, 139, 137, 96, 86, 81, 73, 66, 57.

3-Chloropropyltrimethylsilyl-2-propynyl Bromide (5). Following the procedure above, PPh₃ (5.0 g, 19.1 mmol), CH₂Cl₂ (75 mL), Br₂ (2.9 g, 18.2 mmol) and the silyl ether **3** (5 g, 18 mmol) were combined to yield the desired propargyl bromide **5** (3.3 g, 72%) as a clear oil: IR (CHCl₃, cm⁻¹) 618, 735, 785, 816, 832, 862, 910, 1038, 1205, 1254, 1310, 1413, 1435, 2178, 2905, 2956; ¹H NMR (300 MHz, CDCl₃) δ 0.17 (s, 6 H), 0.70–0.80 (m, 2 H), 1.78–1.92 (m, 2 H), 3.54 (t, *J* = 7 Hz, 2 H), 3.90 (s, 2 H); ¹³C NMR (75 MHz, CDCl₃) δ -2.0, 13.6, 14.6, 27.4, 47.7, 90.8, 101.0; HRMS (EI) *m/z* calcd for (M - CH₃) C₇H₁₁BrClSi (M⁺) 238.9481, found 238.9487; LRMS (EI) *m/z* 239 (M - CH₃), 227, 207, 197, 175, 167, 157, 149, 131, 93, 84, 63.

1-(3-tert-Butyldimethylsilyl-2-propynyl)-6-iodo-1H-pyridin-2-one (7). Iodopyridone **6** (1.5 g, 4.5 mmol), DME (30 mL) and DMF (7.5 mL) were added to a flame-dried flask and the mixture was cooled to 0 °C. NaH (0.19 g, 4.9 mmol) was added portionwise and the mixture was stirred 15 min. Flame-dried LiBr (0.86 g, 9.9 mmol) was added and the reaction was stirred 20 min at 22 °C. Finally, silylpropargyl bromide **4** (2.3 g, 9.9 mmol) was added and the mixture was heated at 60 °C. After 16 h, the mixture was diluted with saturated brine (50 mL) and extracted with EtOAc (8 × 50 mL). The organic layers were combined, dried (MgSO₄) and concentrated. Flash chromatography (95:5 CH₂Cl₂/EtOAc) gave propargylpyridone **7** (1.7 g, 77%) as a white foam: [α]_D²⁰ +58.0 (c 0.2, CHCl₃); IR (CHCl₃, cm⁻¹) 1526, 1648, 1745, 2180, 2859, 2927, 2950, 3548; ¹H NMR (300 MHz, CDCl₃) δ 0.09 (s, 6 H), 0.92 (m, 12 H), 1.79 (m, 2 H), 3.77 (br s, 1 H), 5.00–5.25 (m, 3 H), 5.50 (d, *J* = 16 Hz, 1 H), 7.19 (s, 1H); ¹³C NMR (75 MHz, CDCl₃) δ -4.9, 7.6, 16.6, 26.0, 31.6, 44.5, 66.3, 71.8, 89.4, 98.6, 100.0, 116.5, 118.1, 148.6, 157.9, 173.2; HRMS (EI) *m/z* calcd for C₁₉H₂₆INO₄Si (M⁺) 487.0676, found 487.0679; LRMS (EI) *m/z* 487 (M⁺) 430, 386, 96, 81, 57.

1-[3-(3-Chloropropyl)dimethylsilyl-2-propynyl]-6-iodo-1H-pyridin-2-one (8). Following the procedure for **7**, the

iodopyridone **6** (0.11 g, 0.23 mmol), DME (3.0 mL), DMF (0.75 mL) and NaH (0.01 g, 0.24 mmol) were combined at 0 °C. Flame-dried LiCl (0.02 g, 0.46 mmol) was added and the mixture was stirred vigorously at 22 °C. After 35 min, the silylpropargyl bromide **5** (0.12 g, 0.46 mmol) was added and the reaction mixture was heated at 60 °C for 16 h. Workup and chromatography gave the desired propargylpyridone **8** (0.058 g, 50%) as a 93:7 mixture of alkyl chloride to bromide based on the ¹H NMR spectrum: $[\alpha]_D^{20} +37.7$ (c 0.2, CHCl₃); IR (CHCl₃, cm⁻¹) 1046, 1139, 1158, 1227, 1530, 1651, 1743, 2183, 2959, 3026, 3532; ¹H NMR (300 MHz, CDCl₃) δ 0.20 (s, 6 H), 0.70–0.80 (m, 2 H), 1.01 (t, *J* = 7 Hz, 3 H), 1.70–1.95 (m, 4 H), 3.56 (t, *J* = 7 Hz, 2 H), 3.69 (s, 1 H), 5.08 (d, *J* = 17 Hz, 1 H), 5.16 (d, *J* = 16 Hz, 1 H), 5.20 (d, *J* = 17 Hz, 1 H), 5.54 (d, *J* = 16 Hz, 1 H), 7.23 (s, 1 H); ¹³C NMR (75 MHz, CDCl₃) δ -2.0, 7.8, 13.6, 27.6, 31.7, 44.6, 47.7, 66.4, 71.9, 89.6, 99.2, 100.1, 116.7, 118.3, 148.8, 158.0, 173.3; HRMS (EI) *m/z* calcd for C₂₆H₃₀ClIN₂O₄Si (M⁺) 507.0130, found 507.0124; LRMS (EI) *m/z* 507 (M⁺) 472, 430, 392, 348, 336, 131, 116, 103, 93, 78, 57.

(20S)-7-*tert*-Butyldimethylsilylcampthothecin (12). Propargylpyridone **7** (48.7 mg, 0.1 mmol), benzene (1.4 mL), phenylisonitrile **10** (31.1 mg, 0.3 mmol) and hexamethylditin (50 mg, 0.15 mmol) were added sequentially to a Pyrex pressure tube. The contents were sealed under Ar and irradiated at 70 °C with a 275-W GE Sunlamp. After 9 h, the solvent was evaporated, and the residue was subjected to flash chromatography (CH₂Cl₂/MeOH 96:4, followed by CH₂Cl₂/acetone 9:1) to yield **12** (24.8 mg, 54%) as a light brown solid: $[\alpha]_D^{20} +35.5$ (c 0.2, CHCl₃); IR (CHCl₃, cm⁻¹) 1045, 1158, 1198, 1257, 1555, 1600, 1658, 1741, 2859, 2932, 2960, 2980, 3028; ¹H NMR (300 MHz, CDCl₃) δ 0.69 (s, 6 H), 0.98 (s, 9 H), 1.03 (t, *J* = 7 Hz, 3 H), 1.86 (m, *J* = 7 Hz, 2 H), 3.86 (s, 1 H), 5.29 (d, *J* = 16 Hz, 1 H), 5.31 (s, 2 H), 5.73 (d, *J* = 16 Hz, 1 H), 7.60 (t, *J* = 6 Hz, 1 H), 7.60 (t, *J* = 7 Hz, 1 H), 7.66 (s, 1 H), 7.74 (t, *J* = 7 Hz, 1 H), 8.20 (t, *J* = 8 Hz, 2 H); ¹³C NMR (75 MHz, CDCl₃) δ -0.56, 7.80, 19.2, 27.1, 31.6, 52.4, 66.3, 72.8, 97.7, 118.2, 127.0, 129.5, 129.6, 130.8, 132.7, 136.0, 143.0, 146.4, 148.0, 150.1, 150.6, 157.4, 173.9; HRMS (EI) *m/z* calcd for C₂₆H₃₀N₂O₄Si (M⁺) 462.1974, found 462.1975; LRMS (EI) *m/z* 462 (M⁺), 450, 361, 331, 304, 245, 223, 57.

(20S)-10-Acetoxy-7-*tert*-butyldimethylsilylcampthothecin (13). Following the procedure outlined for **12**, iodopyridone **6** (34.5 mg, 0.071 mmol), *p*-acetoxyphenylisonitrile **11** (48.3 mg, 0.3 mmol), hexamethylditin (35 mg, 0.11 mmol) and benzene (1.3 mL) gave **13** (21.3 mg, 41%) as a tan solid: $[\alpha]_D^{20} +36.2$ (c 0.2, CH₂Cl₂); IR (CHCl₃, cm⁻¹) 1045, 1166, 1195, 1232, 1256, 1371, 1464, 1504, 1557, 1600, 1659, 1742, 2859, 2885, 2902, 2931, 2958, 3000, 3029; ¹H NMR (300 MHz, CDCl₃) δ 0.69 (s, 6 H), 0.90 (s, 9 H), 1.04 (t, *J* = 7 Hz, 3 H), 1.80–2.00 (m, *J* = 7 Hz, 2 H), 2.40 (s, 3 H), 3.81 (s, 1 H), 5.30 (d, *J* = 16 Hz, 1 H), 5.31 (s, 2 H), 5.75 (d, *J* = 16 Hz, 1 H), 7.53 (dd, *J*₁ = 9 Hz, *J*₂ = 2 Hz, 1 H), 7.65 (s, 1 H), 8.08 (d, *J* = 2 Hz, 1 H), 8.21 (d, *J* = 9 Hz, 1 H); ¹³C NMR (125 MHz, CDCl₃) δ -0.6, 7.9, 19.3, 21.5, 27.2, 31.7, 52.5, 66.5, 72.9, 97.7, 118.4, 120.4, 124.8, 132.1, 133.2, 136.7, 142.8, 146.2, 146.4, 149.0, 150.2, 150.8, 157.5, 169.1, 174.1; HRMS (EI) *m/z* calcd for C₂₈H₃₂N₂O₆Si (M⁺) 520.2030, found 520.2014; LRMS (EI) *m/z* 520 (M⁺), 478, 463, 421, 377, 347, 320, 291, 57.

(20S)-7-Chloropropylidimethylsilylcampthothecin (15). Using the conditions described for **12**, iodopyridone **6** (75 mg, 0.15 mmol), phenylisonitrile **10** (45.6 mg, 0.44 mmol) and hexamethylditin (72 mg, 0.22 mmol) in benzene (2 mL) gave **15** (38 mg, 53%), after chromatography (CH₂Cl₂/acetone 20:1), as a tan solid: $[\alpha]_D^{20} +30.8$ (c 0.2, CHCl₃); IR (CHCl₃, cm⁻¹) 1158, 1199, 1220, 1260, 1556, 1600, 1659, 1742, 2937, 2961, 3004, 3016; ¹H NMR (300 MHz, CDCl₃) δ 0.64 (s, 6 H), 0.98 (t, *J* = 7 Hz, 3 H), 1.12–1.25 (m, 2 H), 1.62–1.80 (m, 2 H), 1.80–1.95 (m, *J* = 7 Hz, 2 H), 3.43 (t, *J* = 7 Hz, 2 H), 3.85 (s, 1 H), 5.25 (d, *J* = 16 Hz, 1 H), 5.26 (s, 2 H), 5.69 (d, *J* = 16 Hz, 1 H), 7.58–7.69 (m, 2 H), 7.73 (t, *J* = 8 Hz, 1 H), 8.13 (d, *J* = 8 Hz, 1 H), 8.17 (d, *J* = 8 Hz, 1 H); ¹³C NMR (125 MHz, CDCl₃) δ 0.2, 7.9, 14.7, 27.5, 31.7, 47.4, 51.9, 66.4, 72.8, 97.8, 118.4,

127.6, 127.9, 129.9, 131.3, 132.0, 135.1, 142.5, 146.4, 148.0, 150.2, 151.0, 157.5, 174.0; HRMS (EI) *m/z* calcd for C₂₅H₂₇ClN₂O₄Si (M⁺) 482.1429, found 482.1408; LRMS (EI) *m/z* 482 (M⁺), 453, 438, 425, 382, 361, 275, 149.

(20S)-10-Acetoxy-7-chloropropylidimethylsilylcampthothecin (16). Following the procedure outlined for **12**, iodopyridone **6** (51 mg, 0.1 mmol), *p*-acetoxyphenylisonitrile **11** (48.3 mg, 0.3 mmol) and hexamethylditin (50 mg, 0.15 mmol) in benzene (1.5 mL) gave **16** (24.6 mg, 45%), after chromatography (CH₂Cl₂/acetone 20:1), as a tan solid: $[\alpha]_D^{20} +29.9$ (c 0.2, CHCl₃); IR (CHCl₃, cm⁻¹) 1168, 1195, 1219, 1232, 1259, 1601, 1659, 1743, 3027; ¹H NMR (300 MHz, CDCl₃) δ 0.68 (s, 6 H), 1.05 (t, *J* = 7 Hz, 3 H), 1.19–1.27 (m, 2 H), 1.70–1.80 (m, 2 H), 1.80–1.98 (m, 2 H), 2.42 (s, 3 H), 3.49 (t, *J* = 7 Hz, 2 H), 3.77 (br s, 1 H), 5.31 (d, *J* = 16 Hz, 1 H), 5.31 (s, 2 H), 5.75 (d, *J* = 16 Hz, 1 H), 7.56 (dd, *J*₁ = 9 Hz, *J*₂ = 2 Hz, 1 H), 7.66 (s, 1 H), 8.02 (d, *J* = 2 Hz, 1 H), 8.25 (d, *J* = 9 Hz, 1 H); ¹³C NMR (125 MHz, CDCl₃) δ 0.0, 7.9, 14.5, 21.5, 27.5, 31.7, 47.4, 51.9, 66.4, 72.8, 97.8, 118.5, 118.7, 124.9, 132.3, 132.4, 135.6, 142.2, 145.9, 146.2, 149.2, 150.2, 150.9, 157.5, 169.1, 174.0; HRMS (EI) *m/z* calcd for C₂₇H₂₉ClN₂O₆Si (M⁺) 540.1483, found 540.1479; LRMS (EI) *m/z* 540 (M⁺), 498, 454, 441, 377, 291, 109, 93.

(20S)-10-Hydroxy-7-*tert*-butyldimethylsilylcampthothecin (14). Campthothecin derivative **12** (13.4 mg, 0.026 mmol) was suspended in MeOH (0.2 mL) and H₂O (0.2 mL) and K₂CO₃ (7.2 mg, 0.05 mmol) was added generating a dark solution. After 3 h the mixture was acidified with acetic acid (4 drops), diluted with saturated brine (5 mL) and extracted with EtOAc (10 × 15 mL). The combined organic phase was dried (Na₂SO₄) and evaporated. Purification by preparative TLC (5:1 CH₂Cl₂:acetone) gave **14** (10.6 mg, 85%) as a yellow solid: $[\alpha]_D^{20} +17.4$ (c 0.2, 3:1 CH₂Cl₂/MeOH); ¹H NMR (300 MHz, 3:1 CDCl₃/CD₃OD) δ 0.66 (s, 6 H), 0.88–1.05 (m, 12 H), 1.80–2.00 (m, 2 H), 5.25–5.30 (m, 3 H), 5.70 (d, *J* = 16 Hz, 1 H), 7.37 (dd, *J*₁ = 9 Hz, *J*₂ = 2 Hz, 1 H), 7.54 (d, *J* = 2 Hz, 1 H), 7.60 (s, 1 H), 8.05 (d, *J* = 9 Hz, 1 H); ¹³C NMR (125 MHz, (3:1) CDCl₃:CD₃OD) δ -2.0, 6.7, 18.4, 26.2, 30.4, 52.1, 65.0, 72.4, 97.2, 110.6, 117.3, 121.9, 130.4, 134.2, 135.9, 140.4, 142.1, 145.7, 146.8, 151.1, 156.0, 157.2, 173.2; HRMS (EI) *m/z* calcd for C₂₆H₃₀N₂O₅Si (M⁺) 478.1924, found 478.1947 LRMS (EI) *m/z* 478 (M⁺), 434, 421, 377, 304, 284, 227, 178, 149, 137, 109, 97, 83, 69, 57.

(20S)-10-Hydroxy-7-chloropropylidimethylsilylcampthothecin (17). Following the procedure for **14**, MeOH (0.2 mL), H₂O (0.2 mL) and K₂CO₃ (6.1 mg, 0.04 mmol) was added to a vial containing **16** (11.2 mg, 0.02 mmol). Workup and chromatography (CH₂Cl₂/acetone 5:1) gave **17** (4.8 mg, 44%) as a yellow solid: $[\alpha]_D^{20} +22.5$ (c 0.2, 3:1 CH₂Cl₂/MeOH); ¹H NMR (300 MHz, CDCl₃/CD₃OD) δ 0.65 (s, 6 H), 0.99 (t, *J* = 7 Hz, 3 H), 1.15–1.27 (m, 2 H), 1.65–1.80 (m, 2 H), 1.85–1.97 (m, 2 H), 3.45 (t, *J* = 7 Hz, 2 H), 5.27 (d, *J* = 16 Hz, 1 H), 5.27 (s, 2 H), 5.63 (d, *J* = 16 Hz, 1 H), 7.44 (dd, *J*₁ = 9 Hz, *J*₂ = 2 Hz, 1 H), 7.53 (d, *J* = 2 Hz, 1 H), 7.72 (s, 1 H), 8.12 (d, *J* = 9 Hz, 1 H); ¹³C NMR (125 MHz, CDCl₃/CD₃OD) δ -0.4, 7.6, 14.2, 27.4, 31.3, 47.3, 52.0, 65.9, 72.8, 98.0, 109.7, 118.0, 122.8, 131.2, 133.9, 135.4, 141.1, 141.9, 145.8, 147.2, 151.0, 156.7, 157.6, 173.8; HRMS (EI) *m/z* calcd for C₂₅H₂₇ClN₂O₅Si (M⁺) 498.1378, found 498.1362; LRMS (EI) *m/z* 498 (M⁺), 454, 439, 419, 398, 377, 319, 291, 255, 174, 127, 111, 97, 85, 71, 57.

Chemicals, Blood Components, Drugs, and Drug Stock Solution Preparation. Samples of camptothecin [obtained from the National Cancer Institute (NCI), Bethesda, MD], SN-38 (Yakult Honsha, Tokyo), CPT-11 (Yakult Honsha, Tokyo) and topotecan (NCI, Bethesda, MD) were of high purity (>98%) as determined by HPLC assays with fluorescence detection. Stock solutions of the drugs were prepared in dimethyl sulfoxide (ACS spectrophotometric grade, Aldrich, Milwaukee, WI) at a concentration of 2 × 10⁻³ M and stored in the dark at 4 °C. High-purity water was provided by a Milli-Q UV PLUS. L- α -Dimyristoylphosphatidylcholine (DMPC) and L- α -dimyristoylphosphatidylglycerol (DMPG) were obtained from Avanti Polar Lipids, Alabaster, AL, and were used without further purification. Crystallized HSA of high purity (>97%)

was purchased from Sigma Chemical (St. Louis, MO). Outdated packed red blood cells were obtained from the Kentucky Red Cross and were used without further processing. All other chemicals were reagent grade and were used without further purification.

Characterization of the Model Membrane Interactions of Silatecans Using the Method of Fluorescence Anisotropy Titration. The relative abilities of the new camptothecins to partition into lipid vesicles were determined using the method of fluorescence anisotropy titration. Small unilamellar vesicle (SUV) suspensions were prepared the day of an experiment by the method of Burke et al.²⁰ Briefly, stock lipid suspensions containing 10 mg/mL lipid in phosphate-buffered saline (PBS; pH 7.4) were prepared by Vortex mixing for 5–10 min above the T_m of the lipid. The lipid dispersions were then sonicated using a bath-type sonicator (Laboratory Supplies Co., Hicksville, NY) for 6–8 h until they became optically clear. A decrease in pH from 7.4 to 6.8 was observed for the SUV preparations of DMPG; therefore, the pH of these SUV suspensions was adjusted to 7.4 using small quantities of 1 M NaOH in PBS, followed by additional sonication. Each type of vesicle suspension was annealed for 30 min at 37 °C and then used in an experiment.

Steady-state fluorescence measurements were obtained on a SLM model 9850 spectrofluorometer with a thermostated cuvette compartment. This instrument was interfaced with an IBM PS/2 model 55 SX computer. Excitation and emission spectra were recorded with an excitation resolution of 8 nm and an emission resolution of 4 nm. In all cases spectra were corrected for background fluorescence and scatter from unlabeled lipids or from solvents by subtraction of the spectrum of a blank. Steady-state fluorescence intensity measurements were made in the absence of polarizers. Steady-state anisotropy (a) measurements were determined with the instrument in the "T-format" for simultaneous measurement of two polarized intensities. The alignment of polarizers was checked routinely using a dilute suspension of 0.25 μ M polystyrene microspheres (Polysciences, Inc, Warrington, PA) in water and anisotropy values of >0.99 were obtained. Alternatively, polarizer orientation was checked using a dilute solution of glycogen in water. The anisotropy was calculated from: $a = (I_{VV} - GI_{VH}) / (I_{VV} + 2GI_{VH})$, where $G = I_{HV} / I_{HH}$ and the subscripts refer to vertical and horizontal orientations of the excitation and emission polarizers, respectively.

Anisotropy measurements for camptothecins were conducted using exciting light of 370 nm and long-pass filters on each emission channel in order to isolate the drug's fluorescence signal from background scatter and/or residual fluorescence. All emission filters were obtained from Oriel Corp (Stamford, CT). The combination of exciting light and emission filters allowed adequate separation of fluorescence from background signal. The contribution of background fluorescence, together with scattered light, was typically less than 1% of the total intensity. Since the lactone rings of camptothecin and related congeners undergo hydrolysis in aqueous medium with half-lives of approximately 20 min, all measurements were completed within the shortest possible time (ca. 0.5–1 min) after mixing the drug stock solution with thermally preequilibrated solutions such that the experiments were free of hydrolysis product.

The concentrations of free and bound species of drug in liposome suspensions containing a total drug concentration of 1×10^{-6} M and varying lipid concentrations were completed as described previously.²⁰ All experiments were conducted in glass tubes. The overall association constants are defined as $K = [A_B] / [A_F][L]$, where $[A_B]$ represents the concentration of bound drug, $[A_F]$ represents the concentration of free drug, and $[L]$ represents the total lipid concentration of the sample. Double-reciprocal plots of the binding isotherms $\{1/(\text{bound fraction of drug}) \text{ vs } 1/(\text{lipid})\}$ were linear, and K values were determined from their slopes by the method of linear least-squares analysis. A computer program based on the $K = [A_B] / [A_F][L]$ relationship was written to predict bound drug levels for specified values of K and total drug.

Direct Comparison of the Red Cell Interactions of DB-67 and SN-38 by Fluorescence Spectral Titration. Steady-state fluorescence emission spectra of **14** and SN-38 in suspensions of red cells were obtained using a SLM model 9850 spectrophotometer. Front-face cell geometry was employed in order to optimize signal-to-background ratios. We employed 1×10 -mm quartz cuvettes which were positioned in the sample chamber such that the cuvette surface was mounted 30° from incident to the excitation beam. This angle allowed detection of fluorescence emission from the red cell suspension of high optical density. Spectra were recorded with an excitation resolution of 8 nm and emission resolution of 4 nm. Measurements were performed without an emission polarizer. In all cases, spectra were corrected for background fluorescence and scatter from red cells by subtraction of the spectrum of a blank (i.e. identical red cell suspension but without drug). Spectra were recorded using two drug concentrations: 10 and 50 μ M. In control experiments also employing front-face cell geometry, an emission spectra from 10 μ M **14** in PBS was recorded. In all experiments a wavelength of 370 nm was used for excitation. All measurements were performed at 37 °C.

Kinetics of Lactone Ring Opening. The hydrolysis kinetics of camptothecins in the presence of different blood components were determined by a quantitative C₁₈ reversed-phase high-performance liquid chromatography (HPLC) assay as described previously.^{16,17} The preparation of whole blood and fractionated blood samples was carried out as described previously.¹⁷ HSA stock solutions were prepared in PBS buffer with a final pH of 7.40 ± 0.05 . The HPLC system consisted of a Waters Alliance 2690 separations module with a Waters 474 scanning fluorescence detector. Separations were carried out on a Waters Symmetry-C₁₈ 5- μ m particle size reversed-phase column. To separate the parent from the carboxylate species of these four silatecans, an isocratic mobile phase was employed consisting of varying mixtures of acetonitrile and a 2% (v/v) triethylamine acetate buffer (pH 5.5). Analogue **14** eluted at a ratio of 41% acetonitrile:59% of the triethylamine acetate buffer. Analogue **15** eluted at a ratio of 52% acetonitrile:48% triethylamine acetate buffer. A 35% acetonitrile:65% triethylamine acetate buffer was used for **17**, and a ratio of 58% acetonitrile:42% triethylamine acetate buffer separated the lactone species from the carboxylate species of **12**. The silatecan agents with the 10-hydroxyl groups, **14** and **17**, were detected with a Waters model 474 fluorescence detector at an excitation wavelength of 380 nm and an emission wavelength of 560 nm. Analogues **15** and **12**, which lack the 10-hydroxyl group, were recorded with an excitation wavelength of 365 nm and an emission wavelength of 450 nm. Flow rates of 1 mL/min were employed, and the retention times for the lactone species were approximately 7.0 min. The carboxylate species rapidly eluted at approximately 2.0 min. Fluorescence output signal was monitored and integrated using Millennium³² Chromatography Manager software.

Cell-Free Top1-Mediated DNA Cleavage Assays. These assays were completed according to protocols published.^{22,31–33} Briefly, a 161-bp fragment from pBluescript SK(–) phagemid DNA was restriction digested with *Pvu*II and *Hind*III for 1 h at 37 °C and separated by electrophoresis in a 1% agarose gel. The 161-bp fragment was then eluted from a gel slice using a centricon 50 centrifugal concentrator. Approximately 200 ng of the fragments were 3'-end-labeled at the *Hind*III site via a fill-in reaction with [α -³²P]dCTP, 0.5 mM dATP, dGTP, and dTTP, and 0.5 unit of Klenow fragment. At the end of the labeling reaction the DNA was phenol/chloroform-extracted, ethanol-precipitated, and resuspended in water. Approximately 50 fmol/reaction of DNA substrate was incubated with 5 units of human recombinant top1 or a variety of top1 mutants at 30 °C for 30 min in the presence of the tested analogue. Reactions were terminated by adding SDS (0.5% final concentration). After ethanol precipitation, the samples were suspended in loading buffer and separated in a denaturing gel run and 51 °C. The gels were then dried and visualized by using a phosphorimager and ImageQuant software (Molecular Dynamics).³⁴

Anticancer Activities of 14 Determined in the NCI Human Tumor Cell Line Screens. Briefly, cell suspensions were diluted according to the particular cell type. The expected target cell density (5 000–40 000 cells/well based on cell growth characteristics) was added by pipet (100 μ L) into 96-well microtiter plates. Inoculates were allowed a preincubation period of 24 h at 37 °C for stabilization. Dilutions at twice the intended test concentration were added at time zero in 100- μ L aliquots to each microtiter plate well. All test compounds were prepared in DMSO. Test compounds were evaluated at five 10-fold dilutions; in routine testing, the highest well concentration was 10^{-4} M. Incubations lasted for 48 h in 5% CO₂ and 100% humidity. The cells were assayed by using the sulforhodamine B assay (SRB). A plate reader was used to read the optical densities and a microcomputer processed the optical densities into the special concentration parameters. Additional technical details can be obtained from the Developmental Therapeutics Program of the NCI.

In other experiments, the cytotoxic activities of 14, camptothecin, and SN-38 were characterized in the absence and presence of physiologically relevant concentrations of HSA. MDA-MB-435 S human breast cancer cell lines were used in these assays. In our studies we have found these cells to be tumorigenic with palpable tumors forming at 21–25 days postinjection of 1 million cells into the mammary fat pad of 8–10-week-old female nude mice. The resulting tumors grow progressively and will invade adjacent tissues. These cells, when exposed to a camptothecin analogue, will progress through the G1 and S stages of the cell cycle and arrest in G2/M. From this point the cells undergo apoptosis and/or necrosis and degrade. In our cell viability experiments, cells scored as positive at the completion of a 3-day growth assay are those remaining on the bottom of the culture dish. Since the SRB assay measures protein and is related to cell number (amount of protein per cell), the numbers are intended to reflect the number of cells remaining, but in actuality the numbers reflect the amount of protein on the bottom of the dish which could include both cells and cell fragments. Additionally, cells that are dying or already dead that remain attached are also counted. For cell viability assays exhibiting plateaus in the cell survival profiles, extension of the assays out to 4–5 days would reveal the loss of additional cells.

Acknowledgment. This work was supported by NIH Grants CA63653 (T.G.B.), CA75761 (T.G.B.), and GM31678 (D.C.). The Lucille Markey Trust is acknowledged for their generous support. We gratefully acknowledge Dr. Edward Sausville, Dr. Rao Vishnuvajjala, Ms. Jill Johnson, and the NCI Developmental Therapeutics Program for their valuable assistance and support. S.K. thanks the University of Technology and Agriculture, Bydgoszcz, Poland, for sponsoring his travel to the United States.

Supporting Information Available: Fluorescence emission spectra of 14 and SN-38 is available free of charge via the Internet at <http://pubs.acs.org>.

References

- Pommier, Y.; Pourquier, P.; Fan, Y.; Strumberg, D. Mechanism of action of eukaryotic DNA topoisomerase I and drugs targeted to the enzyme. *Biochim. Biophys. Acta* **1998**, *1400*, 83–105.
- Slichenmyer, W. J.; Rowinsky, E. K.; Donehower, R. C.; Kaufmann, S. H. The current status of camptothecin analogues as antitumor agents. *J. Natl. Cancer Inst.* **1993**, *85*, 271–291.
- Potmesil, M. Camptothecins: from bench research to hospital wards. *Cancer Res.* **1994**, *54*, 1431–1439.
- Takimoto, C. H.; Arbuck, S. G. The Camptothecins. In *Cancer Chemotherapy and Biotherapy*, 2nd ed.; Chabner, B. A., Longo, D. A., Eds.; Lippincott-Raven Publishers: Philadelphia, 1996; pp 463–484.
- Del Bino, G.; Lassota, P.; Darzynkiewicz, Z. The S-phase cytotoxicity of camptothecin. *Exp. Cell Res.* **1991**, *193*, 27–35.
- Hsiang, Y. H.; Lihou, M. G.; Liu, L. F. Arrest of replication forks by drug-stabilized topoisomerase I-DNA cleavable complexes as a mechanism of cell killing by camptothecin. *Cancer Res.* **1989**, *49*, 5077–5082.
- Holm, C.; Covey, J. M.; Kerrigan, D.; Pommier, Y. Differential requirement of DNA replication for the cytotoxicity of DNA topoisomerase I and II inhibitors in Chinese hamster DC3F cells. *Cancer Res.* **1989**, *49*, 6365–6368.
- Giovannella, B. C.; Stehlin, J. S.; Wall, M. E.; Wani, M. C.; Nicholas, A. W.; Liu, L. F.; Silber, R.; Potmesil, M. DNA topoisomerase I-targeted chemotherapy of human colon cancer in xenografts. *Science* **1989**, *246*, 1046–1048.
- Thompson, J.; Stewart, C. F.; Houghton, P. J. Animal models for studying the action of topoisomerase I targeted drugs. *Biochim. Biophys. Acta* **1998**, *1400*, 301–319.
- Jaxel, C.; Kohn, K. W.; Wani, M. C.; Wall, M. E.; Pommier, Y. Structure-activity study of the actions of camptothecin derivatives on mammalian topoisomerase I: evidence for a specific receptor site and a relation to antitumor activity. *Cancer Res.* **1989**, *49*, 1465–1469.
- Hsiang, Y. H.; Liu, L. F.; Wall, M. E.; Wani, M. C.; Nicholas, A. W.; Manikumar, G.; Kirschenbaum, S.; Silber, R.; Potmesil, M. DNA topoisomerase I-mediated DNA cleavage and cytotoxicity of camptothecin analogues. *Cancer Res.* **1989**, *49*, 4385–4389 [published erratum appears in *Cancer Res.* **1989**, *49*, 6868].
- Hsiang, Y. H.; Hertzberg, R.; Hecht, S.; Liu, L. F. Camptothecin induces protein-linked DNA breaks via mammalian DNA topoisomerase I. *J. Biol. Chem.* **1985**, *260*, 14873–14878.
- Hertzberg, R. P.; Caranfa, M. J.; Holden, K. G.; Jakas, D. R.; Gallagher, G.; Mattern, M. R.; Mong, S. M.; Bartus, J. O.; Johnson, R. K.; Kingsbury, W. D. Modification of the hydroxy lactone ring of camptothecin: inhibition of mammalian topoisomerase I and biological activity. *J. Med. Chem.* **1989**, *32*, 715–720.
- Hsiang, Y. H.; Liu, L. F. Identification of mammalian DNA topoisomerase I as an intracellular target of the anticancer drug camptothecin. *Cancer Res.* **1988**, *48*, 1722–1726.
- Fassberg, J.; Stella, V. J. A kinetic and mechanistic study of the hydrolysis of camptothecin and some analogues. *J. Pharm. Sci.* **1992**, *81*, 676–684.
- Burke, T. G.; Mi, Z. Preferential binding of the carboxylate form of camptothecin by human serum albumin. *Anal. Biochem.* **1993**, *212*, 285–287.
- Mi, Z.; Burke, T. G. Differential interactions of camptothecin lactone and carboxylate forms with human blood components. *Biochemistry* **1994**, *33*, 10325–10336.
- Mi, Z.; Burke, T. G. Marked interspecies variations concerning the interactions of camptothecin with serum albumins: a frequency-domain fluorescence spectroscopic study. *Biochemistry* **1994**, *33*, 12540–12545.
- Hochberg, F.; Grossman, S. A.; Mikkelsen, T.; Calabresi, P.; Fisher, J.; Piantadosi, S. For the NABTT CNS Consortium, Baltimore, MD. Efficacy of 9-aminocamptothecin (9-AC) in adults with newly diagnosed glioblastoma multiforme (GBM) and recurrent high grade astrocytomas (HGA). *Proc. Am. Soc. Clin. Oncol.* **1998**, *17*, 388.
- Burke, T. G.; Mishra, A. K.; Wani, M. C.; Wall, M. E. Lipid bilayer partitioning and stability of camptothecin drugs. *Biochemistry* **1993**, *32*, 5352–5364.
- Burke, T. G.; Staubus, A. E.; Mishra, A. K. Liposomal Stabilization of Camptothecin's Lactone Ring. *J. Am. Chem. Soc.* **1992**, *114*, 8318–8319.
- Tanizawa, A.; Fujimori, A.; Fujimori, Y.; Pommier, Y. Comparison of topoisomerase I inhibition, DNA damage, and cytotoxicity of camptothecin derivatives presently in clinical trials. *J. Natl. Cancer Inst.* **1994**, *86*, 836–842.
- Burke, T. G.; Mi, Z. The structural basis of camptothecin interactions with human serum albumin: impact on drug stability. *J. Med. Chem.* **1994**, *37*, 40–46.
- Mi, Z.; Malak, H.; Burke, T. G. Reduced albumin binding promotes the stability and activity of topotecan in human blood. *Biochemistry* **1995**, *34*, 13722–13728.
- Josien, H.; Bom, D.; Curran, D. P.; Zheng, Y. H.; Chou, T. C. 7-Silylcampothecins (Silatecans): A New Family of Camptothecin Antitumor Agents. *Bioorg. Med. Chem. Lett.* **1997**, *7*, 3189–3194.
- Josien, H.; Ko, S.-B.; Bom, D.; Curran, D. P. A General Synthetic Approach to the (20S)-Camptothecin Family of Antitumor Agents by a Regiocontrolled Cascade Radical Cyclization of Aryl Isonitriles. *Chem. Eur. J.* **1998**, *4*, 67–83.
- Curran, D. P.; Liu, H.; Josien, H.; Ko, S.-B. Tandem Radical Reactions of Isonitriles with 2-Pyridonyl and other Aryl Radicals: Scope and Limitations, and a First Generation Synthesis of (racemic) Camptothecin. *Tetrahedron* **1996**, *52*, 11385–11404.
- Pollack, I. F.; Erff, M.; Bom, D.; Burke, T. G.; Strode, J. T.; Curran, D. P. Potent Topoisomerase I Inhibition by Novel Silatecans Eliminates Glioma Proliferation in Vitro and in Vivo. *Cancer Res.* **1999**, *59*, 4898–4905.
- Liu, H.; Ko, S.-B.; Josien, H.; Curran, D. P. Selective N-Functionalization of 6-Substituted-2-pyridones. *Tetrahedron Lett.* **1995**, *36*, 8917–8920.

- (30) Tanizawa, A.; Pommier, Y. Topoisomerase I alteration in a camptothecin-resistant cell line derived from Chinese hamster DC3F cells in culture. *Cancer Res.* **1992**, *52*, 1848–1854.
- (31) Tanizawa, A.; Kohn, K. W.; Pommier, Y. Induction of cleavage in topoisomerase I c-DNA by topoisomerase I enzymes from calf thymus and wheat germ in the presence and absence of camptothecin. *Nucleic Acids Res.* **1993**, *21*, 5157–5166.
- (32) Strumberg, D.; Pommier, Y.; Paull, K.; Jayaraman, M.; Nagafuji, P.; Cushman, M. Synthesis of cytotoxic indenoisoquinoline topoisomerase I poisons. *J. Med. Chem.* **1999**, *42*, 446–457.
- (33) Pourquier, P.; Ueng, L. M.; Fertala, J.; Wang, D.; Park, H. J.; Essigmann, J. M.; Bjornsti, M. A.; Pommier, Y. Induction of reversible complexes between eukaryotic DNA topoisomerase I and DNA-containing oxidative base damages. 7, 8-dihydro-8-oxoguanine and 5-hydroxycytosine. *J. Biol. Chem.* **1999**, *274*, 8516–8523.
- (34) Kohlhausen, G.; Paull, K. D.; Cushman, M.; Nagafuji, P.; Pommier, Y. Protein-linked DNA strand breaks induced by NSC 314622, a novel noncamptothecin topoisomerase I poison. *Mol. Pharmacol.* **1998**, *54*, 50–58.

JM000144O